2020 IEEE International Conference on Robotics and Automation (ICRA)
31 May - 31 August, 2020. Paris, France

Mechanically Programmed Miniature Origami Grippers

Alec Orlofsky*, Chang Liu*, Soroush Kamrava, Ashkan Vaziri, and Samuel M. Felton†

***Abstract*— This paper presents a robotic gripper design that can perform customizable grasping tasks at the millimeter scale. The design is based on the origami string, a mechanism with a single degree of freedom that can be mechanically programmed to approximate arbitrary paths in space. By using this concept, we create miniature fingers that bend at multiple joints with a single actuator input. The shape and stiffness of these fingers can be varied to fit different grasping tasks by changing the crease pattern of the string. We show that the experimental behavior of these strings follows their analytical models and that they can perform a variety of tasks including pinching, wrapping, and twisting common objects such as pencils, bottle caps, and blueberries.**

I. Introduction

Robotic grippers have a large and complex design space. To accomplish the multiple grasping modes necessary for the wide variety of possible tasks [1]–[3], roboticists have tested various approaches including biomimetic designs [4], [5], mechanically adaptive fingers [6], [7], and a combination of multiple, simpler grippers in a single end effector [8]. Advanced grasping techniques often require multiple joints or complex kinematics to achieve different grasps [9].

In contrast, miniature (centimeter- to millimeter-scale) devices rely on simpler designs and alternative fabrication methods. Many miniature grippers operate on a single degree of freedom with simple translational or rotational motions and small strokes [10], [11], limiting their grasp space. Smaller objects necessitate precise movements, but also lower stiffness to avoid damaging fragile components, and these requirements are often mutually exclusive. Soft fluidically actuated fingers [12]–[14] have gentler and more complex motions because of their continuum compliance, but this limits their precision and dexterity. Some grippers have reached smaller scales (micrometer to nanometer) using a global stimulus actuation method [15], [16]. However, these often require specific environments, limiting their functionality.

Origami engineering is well-suited for this application. This paradigm takes inspiration from the eponymous Japanese art form to create complex structures and machines [17], [18]. It has several strengths that can be applied to miniature devices: (1) its planar form factor can facilitate fabrication at the millimeter and micrometer scale [19], [20]; (2) its kinematic complexity and computational design tools allow for complex behaviors [21], [22]; and (3) its inherent compliance makes it compatible with soft and delicate objects [23], [24]. In addition, the planar fabrication techniques enable cheap and rapid prototyping, so such devices could be rapidly redesigned and replaced to match changing functions [25]. Previous origami grippers have demonstrated larger range of motions than traditional designs and lighter weight than soft grippers, but have generally had simple kinematic trajectories [26], [27].

Fig. 1. A miniature gripper based on the origami string.

One example of this paradigm is the origami string – a series of four-crease vertices coupled along a single line [28]. Like the Miura pattern from which it was inspired, the entire string has a single degree of freedom. By appropriately selecting the fold angle and crease pattern at each vertex, these strings can approximate any curve in 3D space [29]. Furthermore, as the structure folds, each vertex passes through a fixed trajectory over time that can also be altered by varying the crease design.

Origami strings are a promising template for miniature grippers for three reasons: (1) because they have a single kinematic degree of freedom, they can be actuated with a single input, minimizing the motor requirements; (2) because they are built from flat sheets they can be fabricated with millimeter-length features [20], [30]; and (3) because of their mechanical programmability, they can achieve the versatility of soft fingers with the constrained kinematics of rigid linkages.

In this paper we demonstrate that origami strings can be used as the basis for functional miniature grippers (Fig. 1). We validate models connecting the kinematic trajectory of these strings with their underlying crease pattern, and show that their stiffness can be similarly altered. We show that these models can be used to design grippers with tailored

Alec Orlofsky, Chang Liu, Soroush Kamrava, Ashkan Vaziri and Samuel M. Felton are with the College of Engineering, Department of Mechanical and Industrial Engineering, Northeastern University, Boston, MA, USA
* Alec Orlofsky and Chang Liu contributed equally to this work
† Corresponding author, s.felton@northeastern.edu

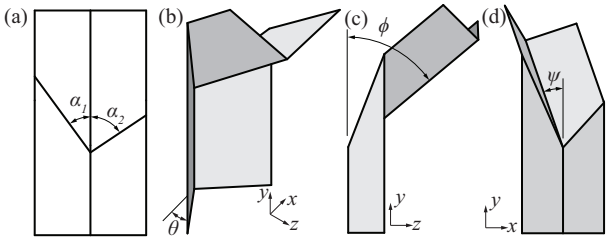

Fig. 2. (a) The Miura vertex consists of four creases: two collinear spinal creases and two peripheral creases at angles α_1 and α_2 from the spine. (b) When folded, the structure bends between the spinal creases. (c) The angular displacement ϕ of the upper spinal crease in the Y-Z plane occurs in all non-trivial vertices. (d) The angular displacement ψ of the upper spinal crease in the X-Y plane only occurs when $\alpha_1 \neq \alpha_2$.

compliance and specific grasping modes including 'pinch', 'wrap', and 'twist'. We then demonstrate the functionality of these grippers by grasping a variety of objects.

II. Background and Model

The Miura vertex is the elemental component of the Miura pattern [31]. It includes four creases, with two collinear spinal creases and two peripheral creases on either side, at angles α_1 and α_2 from the spinal creases (Fig. 2(a)). When folded, the spinal creases have the same angle θ (Fig. 2(b)) and the upper spine exhibits angular displacements ϕ in the Y-Z plane (Fig. 2(c)) and ψ in the X-Y plane (Fig. 2(d)), causing the vertex to effectively 'bend'. These displacements are dependent on α_1, α_2, and θ.

The origami string comprises a series of Miura vertices connected by their spinal creases and sharing a common spinal fold angle θ. The angular displacements (ϕ and ψ) at each vertex are tailored by selecting that vertex's α_1 and α_2. In this way, the string can approximate any path in 3D space by dividing it up into connected line segments (representing the spinal creases between each vertex) and designing the crease pattern to achieve the appropriate bends between the segments [28], [29]. The angles between these vertices can be calculated analytically, and we consider two cases when doing so.

Symmetric vertex: When $\alpha_1 = \alpha_2$, then $\psi = 0$ and an explicit function for ϕ as a function of θ and α has been derived previously [28], [32]. In this situation, the spinal crease can fold completely so that $\theta_{max} = 90°$.

$$\phi = 2\arctan\left(\sin\theta \tan\alpha\right) \tag{1}$$

Asymmetric vertex: When $\alpha_1 \neq \alpha_2$, functions for ϕ and ψ have been derived [33].

$$\phi = \text{arctan2}\left(\frac{2K_1}{\sin\theta}, \left(\frac{K_1}{\sin\theta}\right)^2 + \left(\frac{K_2}{\cos\theta}\right)^2 - 1\right) \tag{2}$$

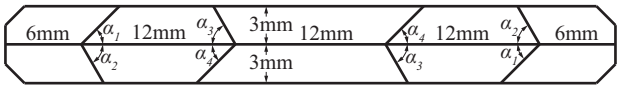

Fig. 3. The origami string used in the gripper and its dimensions.

$$\psi = \arctan\left(\frac{2K_2}{\cos\theta\left[\left(\frac{K_2}{\cos\theta}\right)^2 + \left(\frac{K_1}{\sin\theta}\right)^2 - 1\right]}\right) \tag{3}$$

$$K_1 = \frac{1}{2}\left(\frac{1}{\tan\alpha_1} + \frac{1}{\tan\alpha_2}\right) \tag{4}$$

$$K_2 = \frac{1}{2}\left(\frac{1}{\tan\alpha_1} - \frac{1}{\tan\alpha_2}\right) \tag{5}$$

where arctan2 is the four-quadrant inverse tangent,

$$\text{arctan2}\,(y,x) = \theta \mid [-\pi < \theta \leq \pi \ \wedge \ r > 0 \ \wedge \ x = r\cos\theta \ \wedge \ y = r\sin\theta] \tag{6}$$

When asymmetric, the spinal crease can only fold to θ_{max} [29].

$$\theta_{max} = \frac{\pi}{2} - \frac{1}{2}\arccos\left(\frac{\tan\alpha_1}{\tan\alpha_2}\right) \tag{7}$$

Another way to think about the origami string is as a series of spherical four-bar mechanisms, connected so that the output θ_{out} of each four-bar drives the input θ_{in} of the following one. Because we constrain our design to vertices with collinear spinal creases, $\theta_{in} = \theta_{out}$ for each vertex, resulting in the same θ across the entire string. One consequence of this is that the string has its own maximum fold angle θ_{max} equal to the smallest θ_{max} of each individual vertex.

III. Design and Fabrication

Our system consists of an origami string that functions as the end effector and an actuator assembly that drives the string.

A. Origami String

The origami string can be applied to robotic grippers by considering each vertex a finger joint or knuckle and the spinal creases between them as phalanges. Because

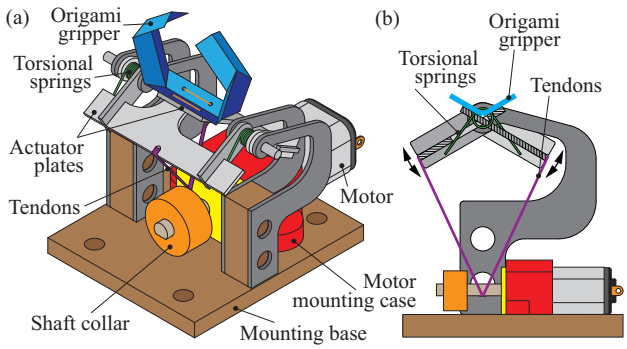

Fig. 4. (a) The actuator assembly folds the origami string at the base segment. (b) A cross-section view of the scissor design.

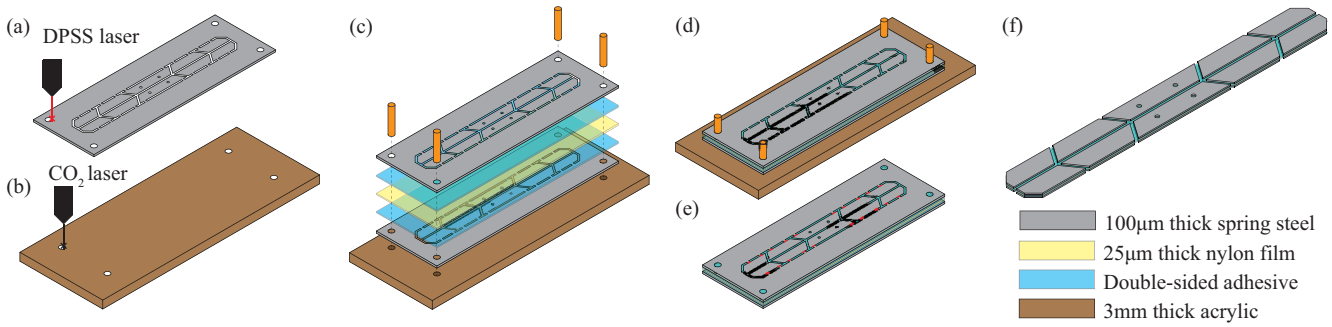

Fig. 5. Fabrication of the origami string. (a) Two sheets of 100 μm thick spring steel were laser machined with thin tabs connecting the plates. (b) A 3 mm thick acrylic base was laser machined. (c) 25 μm thick nylon film was pin-aligned and sandwiched between the steel sheets. All three layers were bonded using double-sided tape. (d) The pins and acrylic base were removed. (e) The tabs were cut using a precision knife. (f) The finished string.

the string has a single degree of freedom, the joints bend simultaneously when the base spinal crease is folded to an angle θ. The magnitude and direction of the joint bending are dependent on the crease patterns at each vertex, defined by α_1 and α_2. Effectively, we can program finger movements that replicate different grasping modes by changing the fingers' fold patterns.

In this paper, each gripper consists of a symmetric origami string that functions as a pair of opposing fingers (Fig. 3). The middle faces form the base segment of the gripper and the spinal crease of this segment is folded directly by the bracket assembly. Two pairs of vertices on either side of the base segment form the two fingers with two joints each; the proximal vertices are adjacent to the base segment, and the distal vertices connect the first and second phalanges.

The string is built as a laminate comprising two layers of 100 μm thick spring steel sandwiched around one layer of 25 μm thick nylon. The facets include all three layers, and the creases are flexural hinges formed by removing the steel, leaving only a 200 μm wide strip of the flexible nylon. Every gripper in this paper has a width of 6 mm, with lengths of 12 mm between each vertex and 6 mm between the last vertex and tip. The α angles vary both in scale and symmetry throughout this paper to customize the gripper for different tasks.

B. Actuator Assembly

The actuator assembly (Fig. 4) folds the base segment of the origami string (center of Fig. 3) and indirectly causes the vertices to bend. This assembly has two 750 μm thick carbon fiber plates that sit flush with the base of the string and rotate about a hinge in a scissor design. The hinge is installed in a 3D-printed mounting base that connects to the robot arm.

To control the motion of the gripper, tendons (coated nylon high-strength thread) are attached to the actuator plates. These tendons are attached to the motor, which is mounted on the base. The tendons and motor are connected such that rotation of the motor shaft will pull the plates together and fold the base segment closed. A 180-degree torsional spring is mounted to the plates to provide an antagonistic torque.

C. Fabrication

The string was built using a laminate process similar to other origami machines [19]. Tee steel layers were cut using an LPKF U4 DPSS laser cutter with thin tabs connecting the plates (Fig. 5(a)). A 3 mm thick acrylic sheet was cut using a ULS CO_2 laser cutter (Fig. 5(b)) for pin alignment in lamination assembly. The nylon was sandwiched and pin-aligned between two sheets of cut structural layers using double-sided tape (Fig. 5(c-d)). Tabs were cut using a precision knife (Fig. 5(e)), releasing the final origami string.

IV. Experiments and Results

A. Kinematic Characterization

To validate our kinematic model, we built six different designs: four symmetrical vertex grippers ($\alpha_i = 30°$, $45°$, $55°$ or $60°$ for $i = 1,2,3,4$) and two asymmetric grippers (one with $\alpha_1 = \alpha_4 = 50°$, $\alpha_2 = \alpha_3 = 60°$; and one with $\alpha_1 = \alpha_4 = 35°$, $\alpha_2 = \alpha_3 = 60°$). We fixed the base angle θ at five different values ($20°$, $30°$, $40°$, $50°$, $60°$) and recorded the gripper position (Fig. 6 shows some of these). We observed that as θ increased, ϕ also increased, closing the grippers. Greater α values resulted in greater ϕ values, causing the gripper to close farther. When $\alpha_1 \neq \alpha_2$, we also observed an offset between the opposing fingertips in the orthogonal direction, indicating nonzero ψ values. Based on the model, we expect to see similar behavior for all vertices where $\alpha_1, \alpha_2 < 90°$.

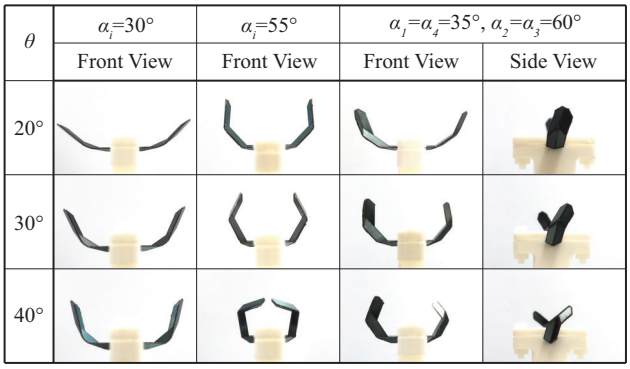

Fig. 6. Three origami string designs with different α values and inputs θ.

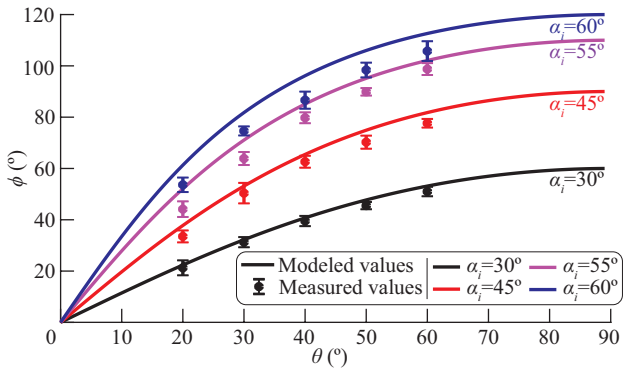

Fig. 7. Vertex displacement ϕ as a function of input fold θ for symmetric strings. Lines indicate model predictions and circles indicate mean experimental results. Black: $\alpha_i = 30°$, red: $\alpha_i = 45°$, magenta: $\alpha_i = 55°$, and blue: $\alpha_i = 60°$. Error bars indicate standard deviation (N=8).

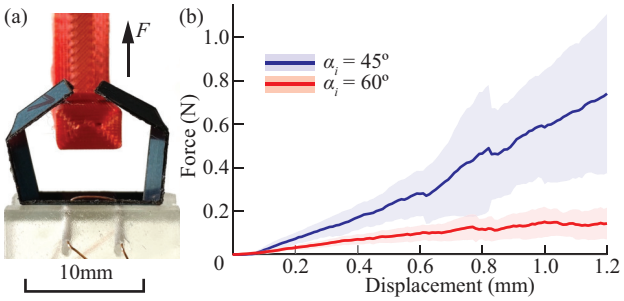

Fig. 9. Stiffness characterization of two grippers with different α and θ values but the same $\phi = 90°$ under no load. (a) Experimental setup. (b) Measured force as a function of vertical displacement. Blue line: $\alpha_i = 45°$, $\theta = 90°$. Red line: $\alpha_i = 60°$, $\theta = 35°$. Shaded areas indicate standard deviation ($N = 6$).

To quantify these results we measured ϕ and ψ of each vertex on two samples (eight vertices total) by importing images of the actuated gripper into Adobe Illustrator, tracing the planar projections of the spinal creases, and calculating the angles between the traces. We plotted those values along with the model predictions as a function of θ (Figs. 7 and 8). These results show that ϕ and ψ mostly match the model predictions. However, there are a few deviations, particularly when $\alpha = 60°$ and the measurements are substantially lower than the predicted values (Fig. 7). This is likely due to inherent compliance in the string combined with substantial stiffness in the hinges. In an ideal string θ is uniform across the string, but in physical specimens the spine unfolds slightly at distal creases, resulting in smaller ϕ values than predicted.

B. Stiffness Characterization

The vertex crease pattern affects the stiffness of each 'joint' as well as its kinematic behavior. The angular displacement at each vertex (defined by ϕ and ψ) is dependent on three independent parameters, θ, α_1, and α_2 so the crease pattern is underconstrained by the kinematic requirements and the same vertex shape can be achieved with many combinations of θ, α_1, and α_2. However, each set of possible design parameters results in a different torsional stiffness at the vertex, allowing us to design for both kinematics and mechanics.

To better understand the mechanics of the origami strings, we tested the stiffness of two gripper designs, one with $\alpha_i = 45°$ and the other with $\alpha_i = 60°$ ($i = 1,2,3,4$). For each gripper, we selected an input θ so that the gripper position ($\phi = 90°$ and $\psi = 0°$ at each vertex) was the same. In this case, grippers with $\alpha_i = 60°$ were fixed to $\theta = 35°$, and grippers with $\alpha_i = 45°$ were fixed to $\theta = 90°$. The gripper was fixed to a base plate under a Mecmesin multitester and the resistive force of a horizontal peg was measured as it moved vertically away from the gripper (Fig. 9(a)). This test was done once per gripper for six different grippers of each design. The resulting force-displacement results are shown in (Fig. 9(b)).

The results show a significantly higher stiffness for grip-

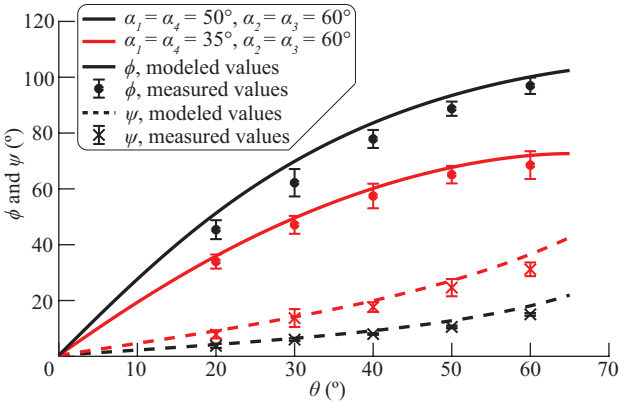

Fig. 8. Vertex displacements ϕ and ψ as a function of input fold θ for asymmetric strings. Solid lines indicate model predictions for ϕ, dashed lines indicate model predictions for ψ, circles indicate mean experimental results for ϕ, and crosses indicate mean experimental results for ψ. Black : $\alpha_1 = \alpha_4 = 50°$, $\alpha_2 = \alpha_3 = 60°$, red: $\alpha_1 = \alpha_4 = 35°$, $\alpha_2 = \alpha_3 = 60°$. Error bars indicate standard deviation (N=8).

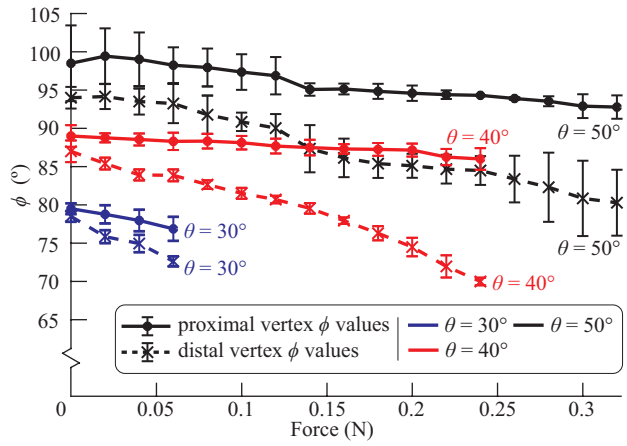

Fig. 10. Vertex displacement ϕ as a function of load. Solid lines and circles represent proximal vertices and dashed lines and crosses represent distal vertices. Blue: $\theta = 30°$, red: $\theta = 40°$, black: $\theta = 50°$. Error bars indicate standard deviation ($N = 2$).

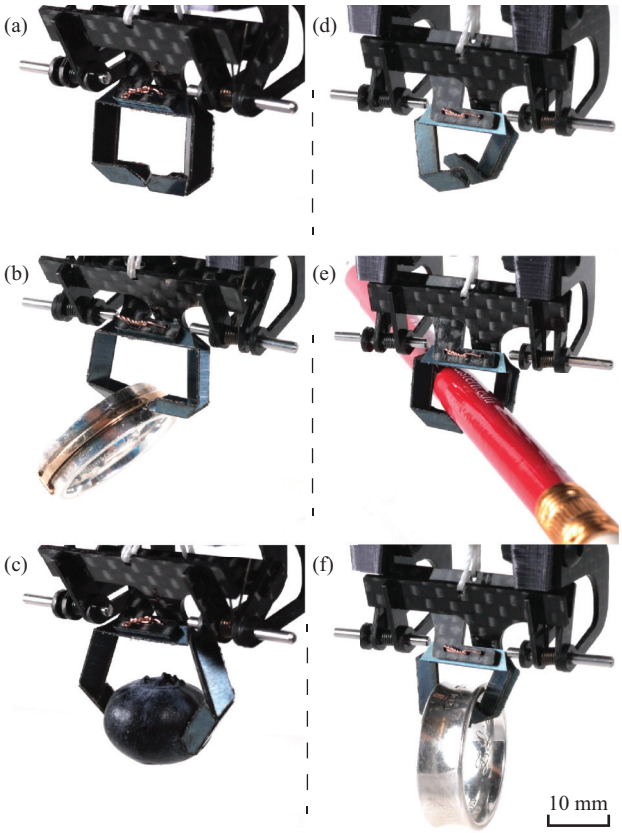

Fig. 11. The pinch gripper closed (a) and grasping a ring (b) and a blueberry (c). The wrap gripper closed (d) and grasping a pencil (e) and a ring (f).

pers with $\alpha_i = 45°$ than for grippers with $\alpha_i = 60°$. This indicates that for a given vertex displacement ϕ, its stiffness can be increased by increasing θ and decreasing α. This makes sense, as a larger θ corresponds to a greater bending moment of the folded structure, resulting in a greater stiffness.

To study how load affects the kinematics, we measured ϕ of both vertices when samples were pulling against an increasing load exerted by the multitester. We used strings with $\alpha_i = 60°$ (the more compliant design from the previous tests) and fixed the base crease angle θ at three different values (30°, 40° and 50°) (Fig. 10). As expected, ϕ decreased approximately linearly due to the string's compliance. In addition, the distal vertices showed a greater change than the proximal vertices under the same load. We believe this is because the deformation at the proximal vertex changed the spinal angle of the following segment and added to the deflection of the distal vertex.

C. Gripper Implementation

To demonstrate the functionality of origami strings as grippers and our ability to program them for different grasping modes, we designed and built three different grippers with three distinct functions: A 'pinch' gripper in which the string tips would come together; a 'wrap' gripper in which the strings would pass each other to circle around an object; and a 'twist' gripper in which the strings were substantially offset to apply a torque around an object. In each case, the gripper was attached to a robot arm, and both the arm and gripper were observed and controlled by a human during operation.

Fig. 12. The wrap gripper lifted a 184 g tea can, the maximum payload demonstrated by these prototypes.

The pinch gripper was designed so that the finger tips came together when the distal segments were roughly parallel, at an input $\theta = 90°$ (Fig. 11(a), Supplemental Video). To accomplish this, $\alpha_i = 55°$ for $i = 1,2,3,4$ (Fig.3). This gripper was capable of grasping and lifting rigid objects with sub-millimeter-scale feature sizes such as a ring with a small extrusion (Fig. 11(b)). It was also relatively compliant, and could lift soft objects (such as a blueberry) without damaging them (Fig. 11(c)).

The wrap gripper was designed so that the string exhibited greater ϕ values at the proximal vertices to increase finger overlap and small deflections in ψ to create an offset between the finger tips, allowing the fingers to pass by each other (Fig. 11 (d), Supplemental Video). To accomplish this, the proximal α values were larger than in the pinch gripper and all vertices were slightly asymmetric. The design consisted of $\alpha_1 = 50°$, $\alpha_2 = 45°$, $\alpha_3 = 65°$, and $\alpha_4 = 70°$. The wrap gripper was well suited to cylindrical objects such as pencils (Fig. 11 (e)) and objects with holes such as rings (Fig. 11 (f)).

The wrap gripper was also well-suited to lifting heavy objects. To test maximum lift capacity, we fabricated a handle with a cross-sectional diameter of 5 mm that we attached to a variety of larger objects to normalize the grasping interface. The same wrap gripper was able to lift several objects including a roll of tape (106g), an orange (167g), and a can of tea (184g) (Fig. 12). The origami string weighed 0.48 g and the entire gripper assembly weighed 26.1 g. Therefore, the gripper demonstrated a strength to weight ratio of 383:1 (7:1 when accounting for the motor and bracket).

The twist gripper was designed to have a substantially larger offset than the wrap gripper, allowing for space

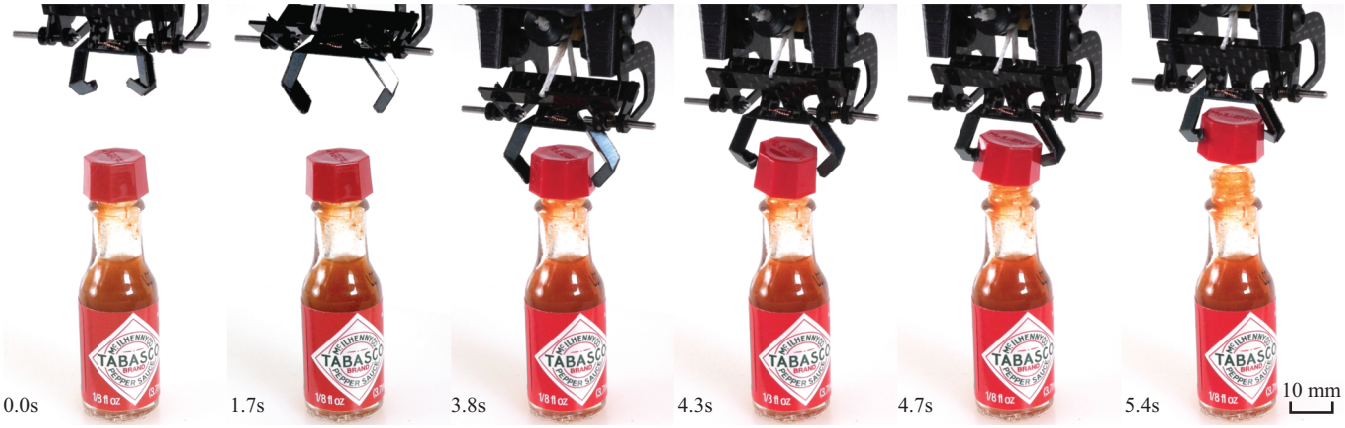

Fig. 13. The twist gripper was applied to unscrewing and lifting the cap of a miniature hot sauce bottle.

between the fingertips as they pass by. In this way the fingers could apply torque to an object. To accomplish this, all vertices were asymmetric, with a larger difference between paired α values than in the wrap gripper: $\alpha_1 = \alpha_4 = 50^\circ$ and $\alpha_2 = \alpha_3 = 60^\circ$. The twist gripper was capable of unscrewing and lifting a bottle cap (Fig. 13, Supplemental Video).

V. Discussion

The results indicate three reasons that the origami string is a promising template for miniature grippers: (1) the laminate fabrication lends itself to millimeter-scale features; (2) the origami pattern can achieve constrained and tunable kinematics driven by a single actuator; and (3) the compliance of the structure can be similarly adjusted for handling delicate objects. Although each sample could only perform a single grasp, the fabrication process and geometric model enable rapid design and fabrication, so new end effectors could be quickly designed, built, and installed at relatively low cost.

We observed some discrepancies between our geometric models and experimental results. We believe this is due to the flexibility of the facets relative to the hinges. Future work could optimize the physical specimen to behave more like the ideal model, or improve the model to account for the compliance. This research could also be used to understand the relationship between fold pattern and joint stiffness. Our results show that stiffness can be adjusted through the fold pattern but we did not identify the underlying reasons. We believe it to be some combination of twisting in the facets and off-axis bending or stretching at the hinges, but the relative contributions of each are likely due to the materials and fabrication process.

These experiments also revealed limitations in the actuation range of origami strings with inherent compliance. As Equation 7 states, asymmetric vertices have a maximum fold angle θ_{max}. For the asymmetric fingers demonstrated here with $\alpha_1 = 35^\circ$ and $\alpha_2 = 60^\circ$, $\theta_{max} = 57^\circ$. Because one string shares a single value θ across all vertices, θ_{max} for the string is the minimum θ_{max} among its vertices. However, even in symmetric strings we couldn't fold more than $\theta_{max} \approx 80^\circ$ without causing substantial deformation and delamination in the structures. In addition, all the strings we tested had an effective minimum input angle θ_{min}, which was typically around 15°. Smaller values of θ would cause the vertices to approach their singularity, making them vulnerable to snap-through that would change the gripper kinematics.

One practical limitation to the design space is the total number of vertices that can fit in a physical specimen. An ideal origami string can approximate any path in 3D space by chaining together an arbitrary number of vertices. However, the weight and compliance of physical specimens result in deformation along the strings. This deformation becomes substantial with four or more vertices and our assumption that θ is uniform is no longer accurate. However, if the design, materials, and fabrication of origami strings could be optimized to allow for 10 or more vertices, we could build end effectors that resemble e.g. tentacles.

Another avenue of future research is making strings that can transform between different grasping modes. Previous research has shown that origami mechanisms can change their configuration by switching the fold direction of their hinges [34]. This can be accomplished without additional motors, either through dynamic transformation [35] or by applying an external force. Future research could study the functionality of miniature grippers designed for transformation.

Another design limitation was that we only considered vertices with collinear spinal creases. However, it is possible to make strings from four-edge vertices without collinear creases, greatly expanding the design space. Such vertices may allow for increased control over the stiffness or a greater range of kinematic behaviors with a fixed number of vertices. However, the geometric equations governing their kinematics become more complex and many assumptions (such as a single θ at all spinal hinges) are no longer applicable, making the design process more challenging.

Acknowledgment

This work was funded by Northeastern University.

References

[1] T. Feix, R. Pawlik, H.-B. Schmiedmayer, J. Romero, and D. Kragic, "A comprehensive grasp taxonomy," in *Robotics, science and systems:*

workshop on understanding the human hand for advancing robotic manipulation, vol. 2, no. 2.3, 2009, pp. 2–3.

[2] I. M. Bullock, R. R. Ma, and A. M. Dollar, "A hand-centric classification of human and robot dexterous manipulation," *IEEE transactions on Haptics*, vol. 6, no. 2, pp. 129–144, 2012.

[3] F. Suárez-Ruiz, I. Galiana, Y. Tenzer, L. P. Jentoft, R. D. Howe, and M. Ferre, "Grasp mapping between a 3-finger haptic device and a robotic hand," in *International Conference on Human Haptic Sensing and Touch Enabled Computer Applications*. Springer, 2014, pp. 275–283.

[4] N. A. Radford, P. Strawser, K. Hambuchen, J. S. Mehling, W. K. Verdeyen, A. S. Donnan, J. Holley, J. Sanchez, V. Nguyen, L. Bridgwater *et al.*, "Valkyrie: NASA's first bipedal humanoid robot," *Journal of Field Robotics*, vol. 32, no. 3, pp. 397–419, 2015.

[5] V. Bundhoo and E. J. Park, "Design of an artificial muscle actuated finger towards biomimetic prosthetic hands," in *ICAR'05. Proceedings., 12th International Conference on Advanced Robotics, 2005.* IEEE, 2005, pp. 368–375.

[6] A. M. Dollar and R. D. Howe, "The SDM hand: A highly adaptive compliant grasper for unstructured environments," in *Experimental Robotics*. Springer, 2009, pp. 3–11.

[7] K. C. Galloway, K. P. Becker, B. Phillips, J. Kirby, S. Licht, D. Tchernov, R. J. Wood, and D. F. Gruber, "Soft robotic grippers for biological sampling on deep reefs," *Soft robotics*, vol. 3, no. 1, pp. 23–33, 2016.

[8] C. Hernandez, M. Bharatheesha, W. Ko, H. Gaiser, J. Tan, K. van Deurzen, M. de Vries, B. Van Mil, J. van Egmond, R. Burger *et al.*, "Team Delft's robot winner of the Amazon picking challenge 2016," in *Robot World Cup*. Springer, 2016, pp. 613–624.

[9] N. Banerjee, X. Long, R. Du, F. Polido, S. Feng, C. G. Atkeson, M. Gennert, and T. Padir, "Human-supervised control of the atlas humanoid robot for traversing doors," in *2015 IEEE-RAS 15th International Conference on Humanoid Robots (Humanoids)*. IEEE, 2015, pp. 722–729.

[10] M. Mertmann and E. Hornbogen, "Grippers for the micro assembly containing shape memory actuators and sensors," *Le Journal de Physique IV*, vol. 7, no. C5, pp. C5–621, 1997.

[11] N. K. Sodavaram and K. M. Arif, "A compact stepper motor actuated disposable microgripper," *International Journal of Precision Engineering and Manufacturing*, vol. 17, no. 10, pp. 1359–1364, 2016.

[12] K. Suzumori, S. Iikura, and H. Tanaka, "Development of flexible microactuator and its applications to robotic mechanisms," in *Proceedings. 1991 IEEE International Conference on Robotics and Automation*. IEEE, 1991, pp. 1622–1627.

[13] S. Wakimoto, K. Ogura, K. Suzumori, and Y. Nishioka, "Miniature soft hand with curling rubber pneumatic actuators," in *2009 IEEE International Conference on Robotics and Automation*. IEEE, 2009, pp. 556–561.

[14] G. Udupa, P. Sreedharan, P. Sai Dinesh, and D. Kim, "Asymmetric bellow flexible pneumatic actuator for miniature robotic soft gripper," *Journal of Robotics*, vol. 2014, 2014.

[15] E. Diller and M. Sitti, "Three-dimensional programmable assembly by untethered magnetic robotic micro-grippers," *Advanced Functional Materials*, vol. 24, no. 28, pp. 4397–4404, 2014.

[16] K. Malachowski, M. Jamal, Q. Jin, B. Polat, C. J. Morris, and D. H. Gracias, "Self-folding single cell grippers," *Nano letters*, vol. 14, no. 7, pp. 4164–4170, 2014.

[17] T. Tachi, "Freeform variations of origami," *J. Geom. Graph*, vol. 14, no. 2, pp. 203–215, 2010.

[18] S. J. Callens and A. A. Zadpoor, "From flat sheets to curved geometries: Origami and kirigami approaches," *Materials Today*, vol. 21, no. 3, pp. 241–264, 2018.

[19] J. P. Whitney, P. S. Sreetharan, K. Y. Ma, and R. J. Wood, "Pop-up book MEMS," *Journal of Micromechanics and Microengineering*, vol. 21, no. 11, p. 115021, 2011.

[20] J. Rogers, Y. Huang, O. G. Schmidt, and D. H. Gracias, "Origami MEMS and NEMS," *MRS Bulletin*, vol. 41, no. 2, pp. 123–129, 2016.

[21] E. D. Demaine and J. O'Rourke, *Geometric folding algorithms: linkages, origami, polyhedra*. Cambridge university press, 2007.

[22] T. Tachi, "Origamizing polyhedral surfaces," *IEEE transactions on visualization and computer graphics*, vol. 16, no. 2, pp. 298–311, 2009.

[23] L. Paez, G. Agarwal, and J. Paik, "Design and analysis of a soft pneumatic actuator with origami shell reinforcement," *Soft Robotics*, vol. 3, no. 3, pp. 109–119, 2016.

[24] S. Li, H. Fang, S. Sadeghi, P. Bhovad, and K.-W. Wang, "Architected origami materials: How folding creates sophisticated mechanical properties," *Advanced Materials*, vol. 31, no. 5, p. 1805282, 2019.

[25] C. D. Onal, M. T. Tolley, R. J. Wood, and D. Rus, "Origami-inspired printed robots," *IEEE/ASME transactions on mechatronics*, vol. 20, no. 5, pp. 2214–2221, 2014.

[26] B. J. Edmondson, L. A. Bowen, C. L. Grames, S. P. Magleby, L. L. Howell, and T. C. Bateman, "Oriceps: Origami-inspired forceps," in *ASME 2013 conference on smart materials, adaptive structures and intelligent systems*. American Society of Mechanical Engineers Digital Collection, 2013.

[27] Z. Kan, Y. Zhang, Y. Yang, Y. A. Tse, and M. Y. Wang, "An origami-inspired monolithic soft gripper based on geometric design method," in *2019 2nd IEEE International Conference on Soft Robotics (RoboSoft)*. IEEE, 2019, pp. 470–476.

[28] S. Kamrava, D. Mousanezhad, S. M. Felton, and A. Vaziri, "Programmable origami strings," *Advanced Materials Technologies*, vol. 3, no. 3, p. 1700276, 2018.

[29] S. Kamrava, R. Ghosh, Y. Yang, and A. Vaziri, "Slender origami with complex 3D folding shapes," *EPL (Europhysics Letters)*, vol. 124, no. 5, p. 58001, 2018.

[30] R. J. Wood, S. Avadhanula, R. Sahai, E. Steltz, and R. S. Fearing, "Microrobot design using fiber reinforced composites," *Journal of Mechanical Design*, vol. 130, no. 5, p. 052304, 2008.

[31] K. Miura, "Method of packaging and deployment of large membranes in space," *Title The Institute of Space and Astronautical Science Report*, vol. 618, p. 1, 1985.

[32] S. Miyashita, C. D. Onal, and D. Rus, "Multi-crease self-folding by global heating," *Artificial life*, vol. 21, no. 4, pp. 398–411, 2015.

[33] S. Kamrava, C. Liu, A. Q. Orlofsky, A. Vaziri, and S. M. Felton, "A closed-form solution for the kinematics of asymmetric miura vertices," *arXiv preprint arXiv:2001.07657*, 2020.

[34] F. Zuliani, C. Liu, J. Paik, and S. M. Felton, "Minimally actuated transformation of origami machines," *IEEE Robotics and Automation Letters*, vol. 3, no. 3, pp. 1426–1433, 2018.

[35] C. Liu and S. M. Felton, "Transformation dynamics in origami," *Physical review letters*, vol. 121, no. 25, p. 254101, 2018.